Electronic Supplementary Material (ESI) for Journal of Materials Chemistry A.
This journal is © The Royal Society of Chemistry 2016

Supplementary information

Insights into Electronic Bands of $WO_3/BiVO_4/TiO_2$, Revealing High Solar Water Splitting Efficiency

Shankara S. Kalanur, Il-Han Yoo, Jucheol Park and Hyungtak Seo,*

E-mail: hseo@ajou.ac.kr

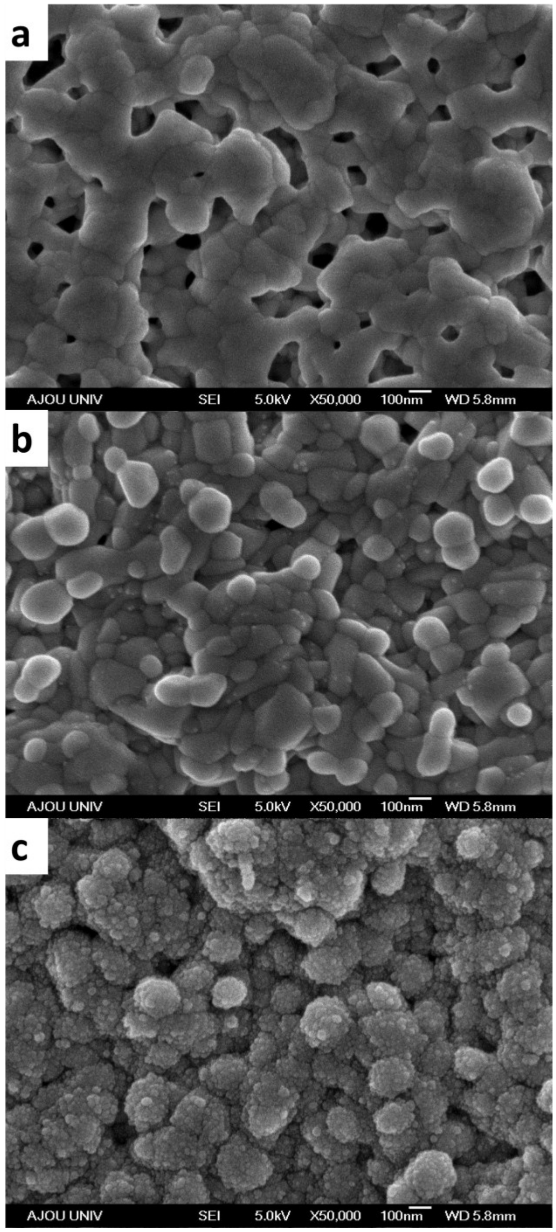

Figure S1. (a) Top view SEM image of $BiVO_4$ deposited on WO_3 without the organic binder ethyl cellulose and (b) with ethyl cellulose. (c) 5-nm-thick TiO_2 electrochemically deposited onto $WO_3/BiVO_4$.

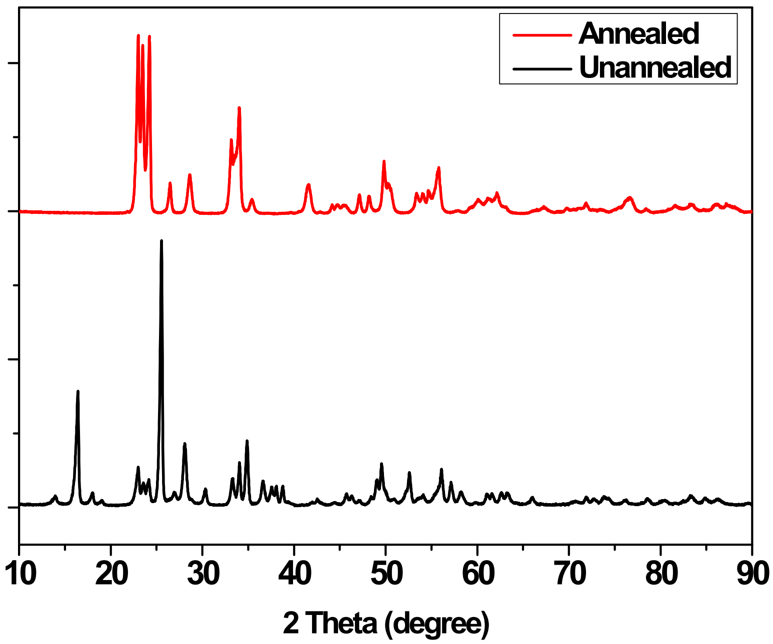

Figure S2. XRD patterns for the as-synthesized orthorhombic (black line) and annealed (500 °C) monoclinic WO_3 nanostructures.

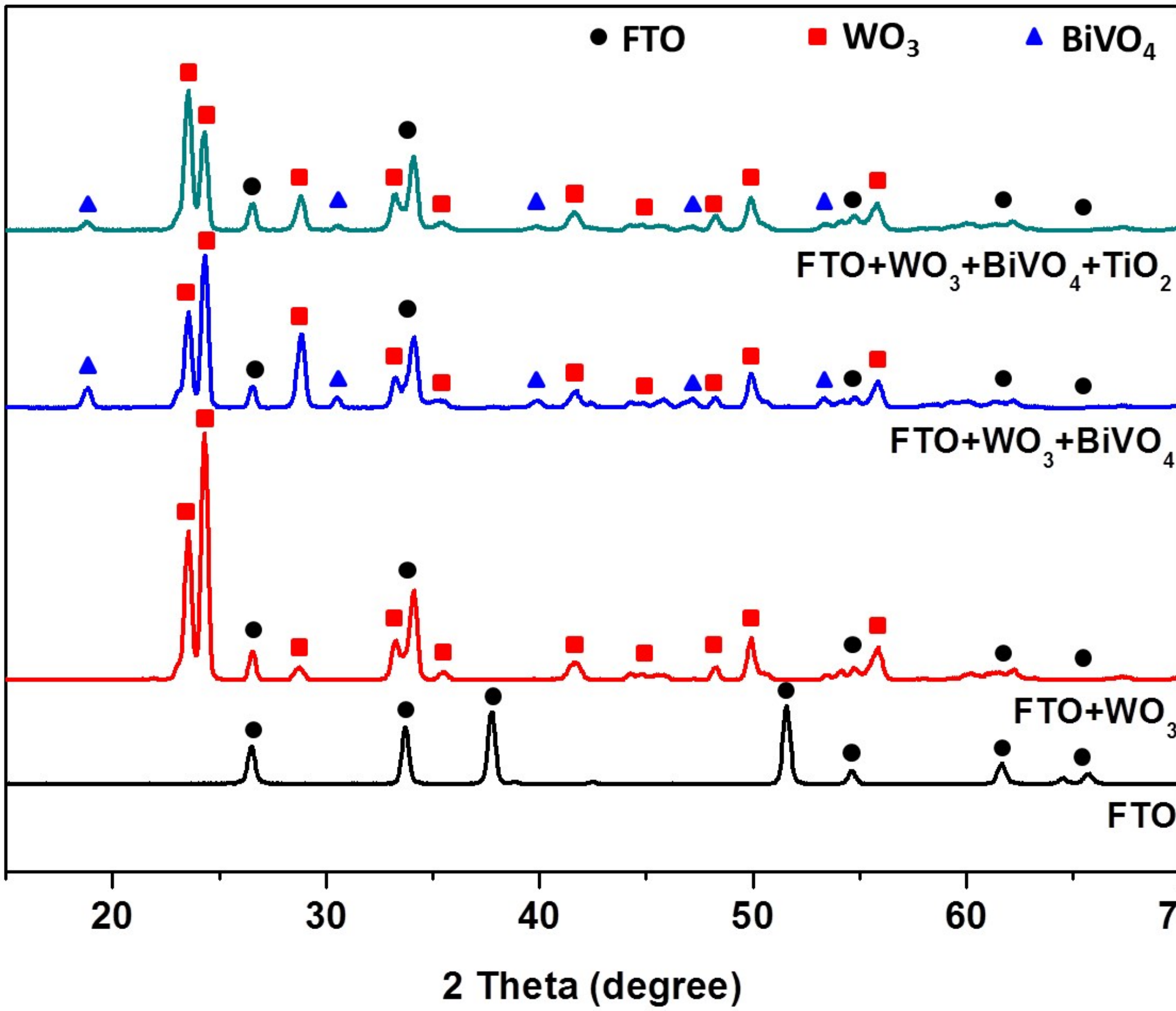

Figure S3. XRD patterns for FTO (black line), FTO/WO_3 (red line), FTO/WO_3/$BiVO_4$ (blue line), and FTO/WO_3/$BiVO_4$/TiO_2 (green line). The peaks for FTO, WO_3, and $BiVO_4$ are indicated with black circles, red squares, and blue triangles, respectively. TiO_2 peaks could not be seen, most probably due to the thinness of the TiO_2 layer and the high intensity of the peaks for the other materials.

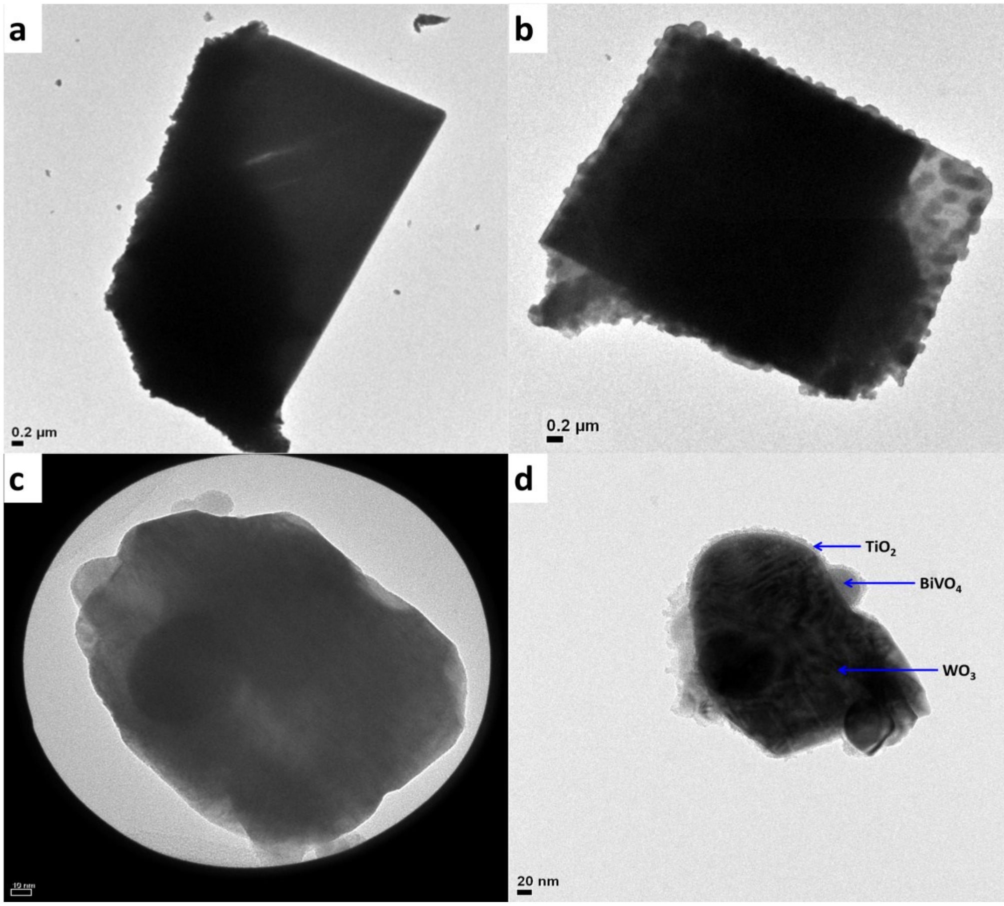

Figure S4. TEM images of the WO_3 plate structures (a) without and (b) with $BiVO_4$. TEM images of the porous WO_3 structures (c) without and (d) with $BiVO_4$ and TiO_2.

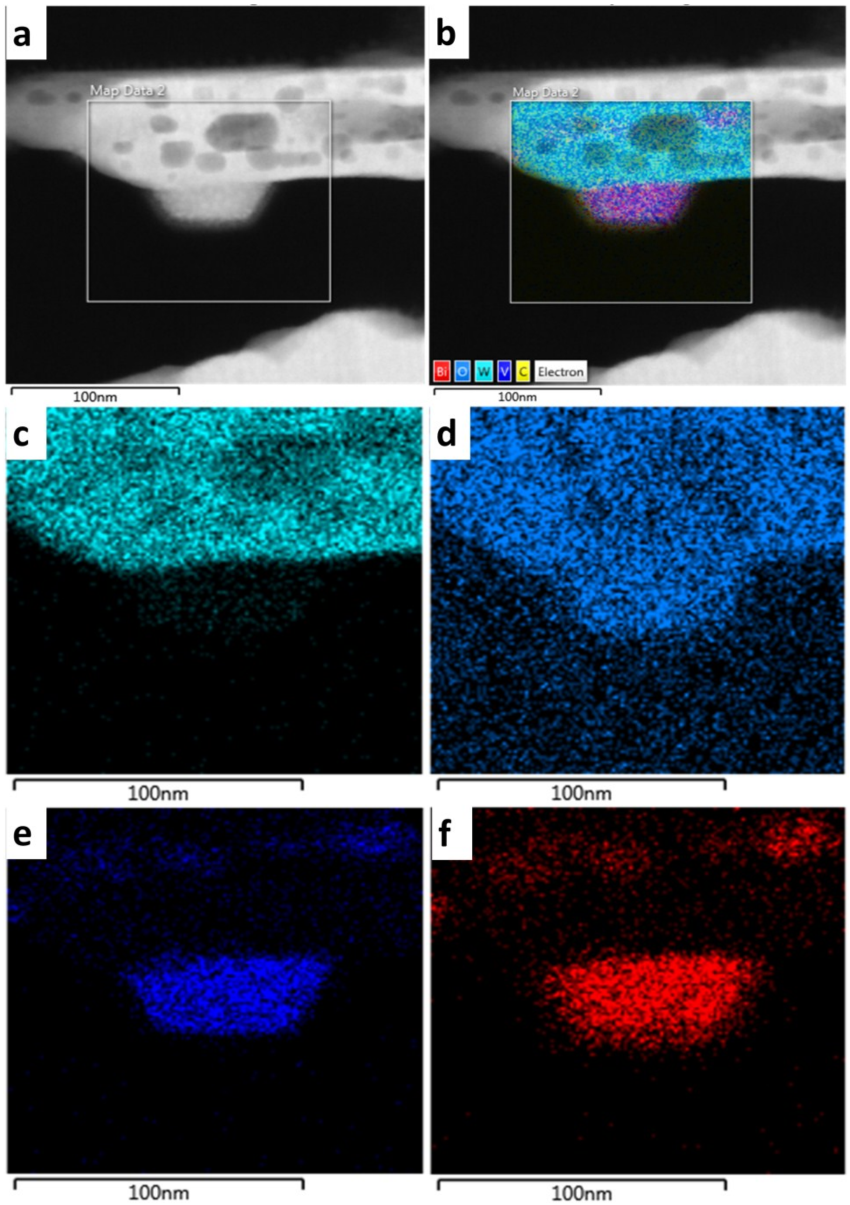

Figure S5. Elemental mapping for $WO_3/BiVO_4$ showing the distribution each element, indicated by different colors. (a) STEM image of $WO_3/BiVO_4$ in the selected area. (b) Mapped elements in the selected area. Elements (c) W, (d) O, (e) Bi, and (f) V are represented by different colors.

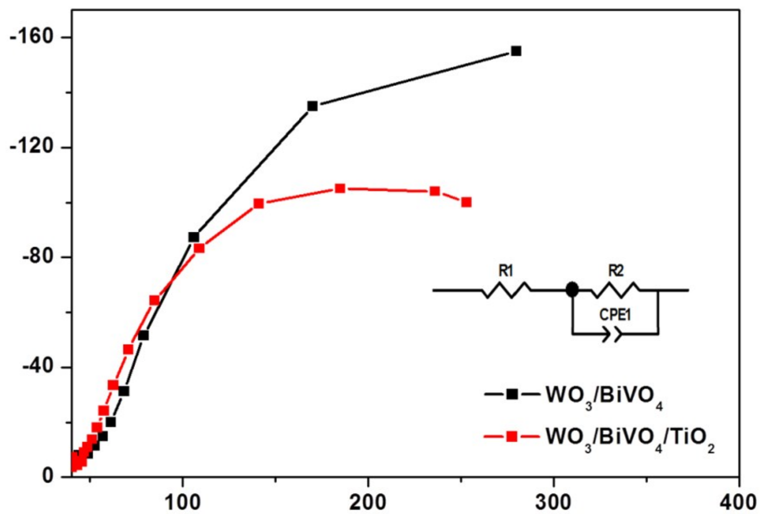

Figure S6. Nyquist plots obtained at 1.23 V Vs RHE under illumination for the $WO_3/BiVO_4$ and $WO_3/BiVO_4/TiO_2$. R1 is the solution resistance; R2 is the charge transfer resistance between electrode and electrolyte. CPE1 is the constant phase element between electrode/electrolyte.

Photoanode	R1	R2	CPE1	n
$WO_3/BiVO_4$	41.58	400.2	$4.303x10^{-5}$	0.9763
$WO_3/BiVO_4/TiO_2$	51.11	267.7	$3.694\ x10^{-5}$	0.9763

Table S1. R1 is the solution resistance, R2 is the charge transfer resistance between electrode and electrolyte. CPE1 is the constant phase element between electrode/electrolyte. The impedance results showed that R2 and CPE1 decreased with the addition of TiO_2 layer.

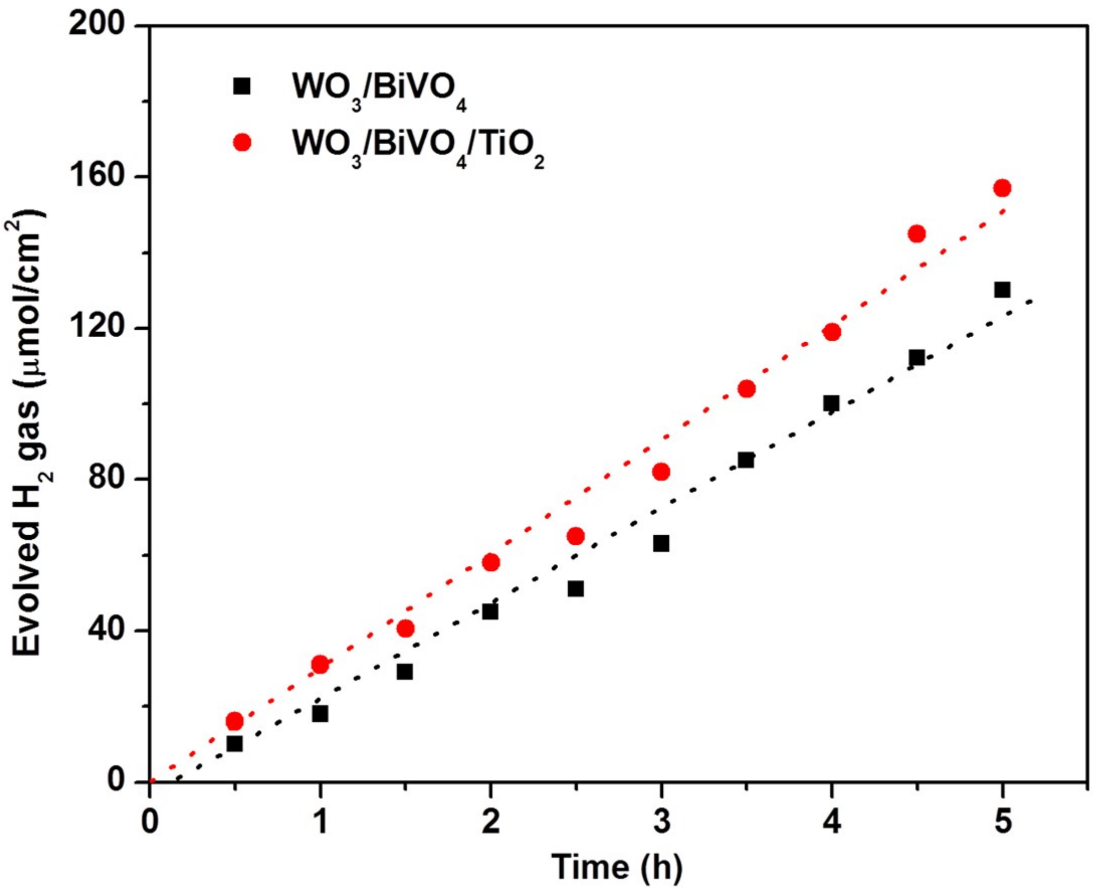

Figure S7. Time course curves of H_2 evolution (at 0.8 V vs Ag/AgCl) over the $WO_3/BiVO_4/TiO_2$ photoanode in a three-electrode cell under simulated sunlight.

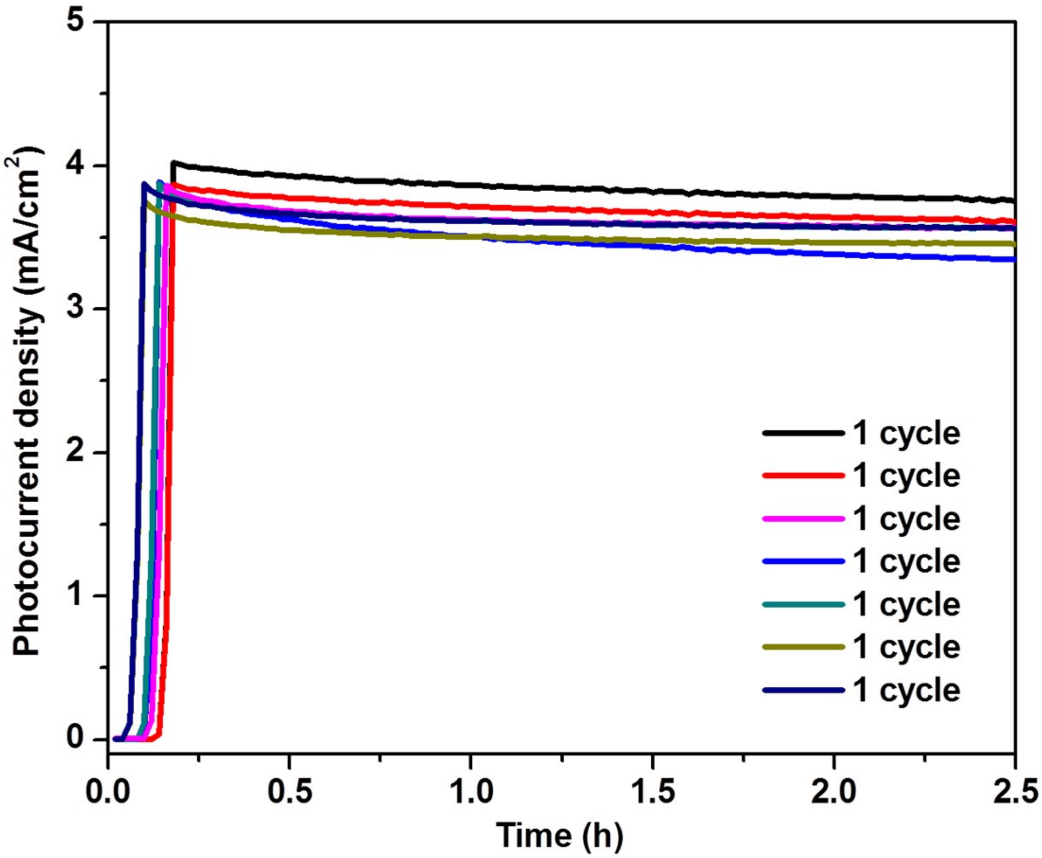

Figure S8. I-V characteristics of $WO_3/BiVO_4/TiO_2$ photoanode measure at 1.23 V vs RHE at different cycles.

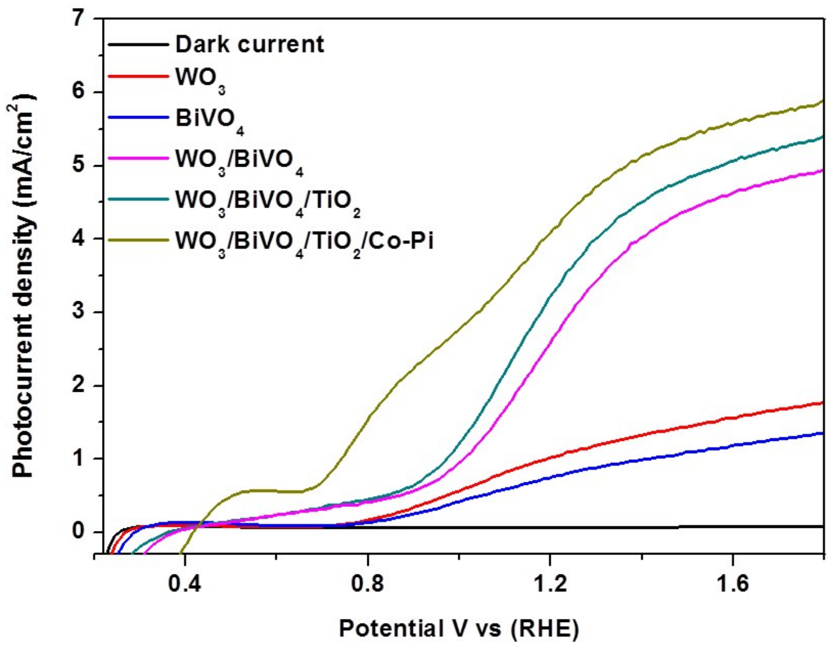

Figure S9. J-V plots for WO_3, $BiVO_4$, $WO_3/BiVO_4$, $WO_3/BiVO_4/TiO_2$, and $WO_3/BiVO_4/TiO_2$/Co-Pi under simulated solar illumination in a 0.1 M Na_2SO_4 electrolyte.

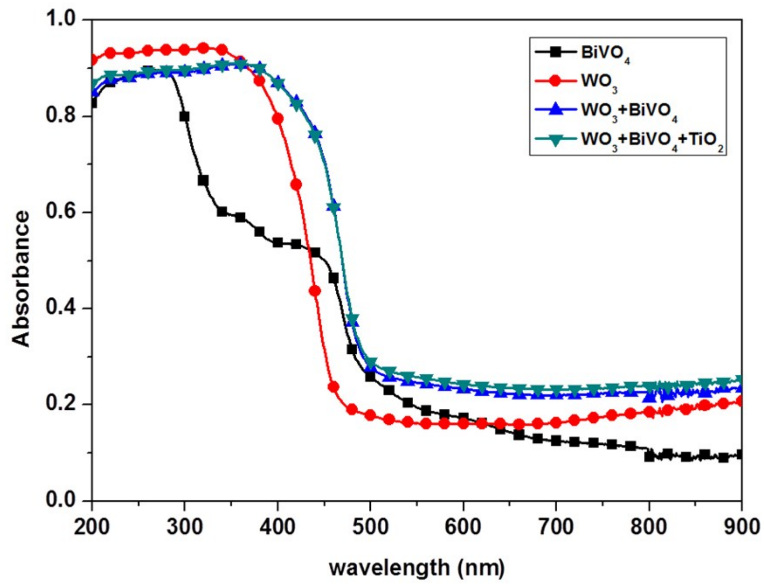

Figure S10. UV-Vis absorption curves for WO_3, $BiVO_4$, $WO_3/BiVO_4$, and $WO_3/BiVO_4/TiO_2$.

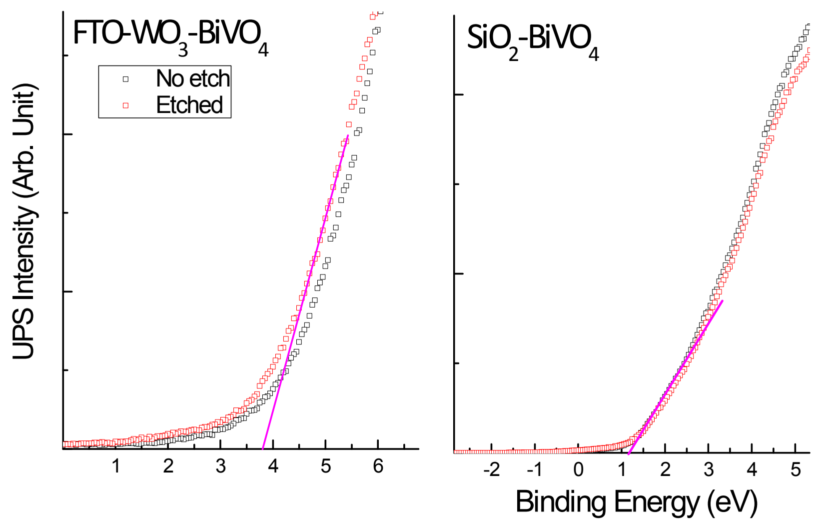

Figure S11. VBM of BiVO4 is ~ 1.2 eV which is in consistent with XPS results. This indicates mid-gap like character of $BiVO_4$ surface based on E_F position.

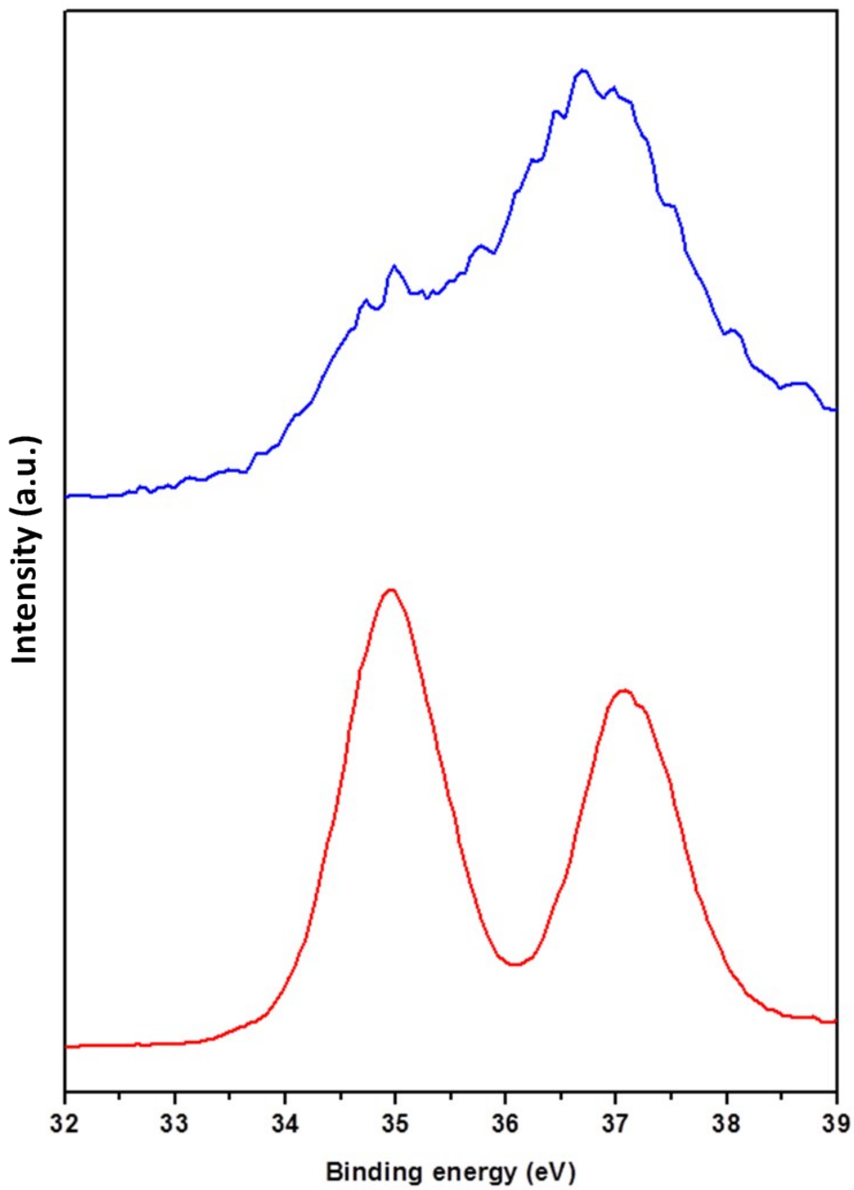

Figure S12. High-resolution XPS spectra of the W4f core level before (red line) and after (blue line) forming a heterojunction with $BiVO_4$.